MODELING BENT RADIO JETS:
ANOTHER PROBE OF THE CENTRAL ENGINE

P.A. HUGHES, M.F. ALLER and H.D. ALLER
Astronomy Department, University of Michigan

Abstract. We present a model for curved parsec-scale jets that includes most of the key radiation physics and relativity, but which is simple enough to allow an exploration of diverse geometries and flow parameters.

1. Introduction

Recent VLBI observations have shown that parsec-scale jets commonly exhibit bent, sometimes complex, and/or changing, morphology. Although enhanced by line-of-sight projection, there must be a nonlinearity of the flow. The strong sensitivity of the total and polarized fluxes to flow speed and orientation (through Doppler frequency shift, Doppler boost, aberration and time delays) means that modeling *must* allow for such flow nonlinearity and *may* in fact elucidate the flow geometry. Once determined, the flow geometry should give a strong indication of the origin of nonlinearity, *e.g.*, precession of the central engine; an ambient pressure gradient; an ambient density gradient, or 'clouds'; back action of a cocoon flow on the jet; Kelvin-Helmholtz instability – and hence probe the nature of the flow *and the ambient conditions* on parsec and sub-parsec scales. This article addresses a method of modeling nonlinear flows.

Fitting multi-frequency, multi-epoch total and polarized flux data calls for detailed radiation transfer calculations (Gómez, Alberdi & Marcaide 1993; Hughes, Aller & Aller 1989; Jones 1988; van der Walt 1993). However, this procedure is too computationally intensive to admit extensive exploration of parameter space. Something simpler – ideally, interactive – but quantitative is needed (Marscher & Zhang 1991; Steffen 1992). We describe a model that includes most of the key radiation physics and relativity, albeit in a simple way, and provides on-the-fly maps and light curves. We illustrate the usage of the model by interpreting the observations of 4C 39.25. The model enables us to reproduce/understand the *general* features of this source: namely the stationary and propagating components seen on VLBI maps and the derived β_{app}; and the profiles and percentage polarization exhibited by single dish data.

2. The Model

The geometry is an arbitrary locus on which are 'threaded' circularly-cylindrical pills of increasing radius and diminishing field and particle energy density.
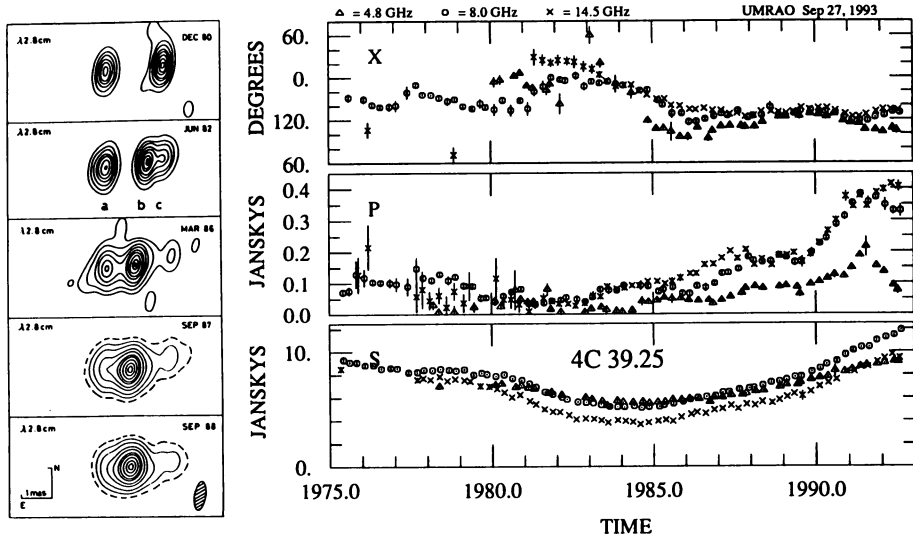
233

Fig. 1. Maps and light curves for 4C 39.25. The panels from bottom to top are: total flux, polarized flux and PA of the electric vector. Each point is a tri-monthly average.

The total and polarized fluxes of *each* pill are calculated assuming a homogeneous synchrotron plasma, and these are converted to intensities by 'distributing' the emission over the projected area of the pill.

A 'superluminal' component may be generated by specifying a strength and extent of shocked jet. The jump conditions are used to determine the state of the shocked flow, and the polarized emission is associated with a compressed tangled magnetic field.

For an arbitrarily oriented observer, the spectral shift, Doppler boost, aberration (which in part determines the degree of observed polarization) and time delay with respect to the jet 'base' are computed for each pill. The emissivity in both quiescent and shocked parts of the flow takes account of these effects.

For each pill a set of 'weights' is computed, associated with the degree of overlap of juxtaposed pills. Maps and light curves are made using the information contained in these weights and a measure of the opacity of each pill, using complex polarization to correctly sum the individual polarized fluxes.

The calculations are 'packaged' to provide an interactive display, wherein a source may be rotated, parameters (*e.g.*, the rate of decline of the emissivity along the jet, the 'observing' frequency, the quiescent flow Lorentz factor and the direction of the shock) changed, and shocks propagated with on-the-fly map and light curve generation (see Fig. 3).
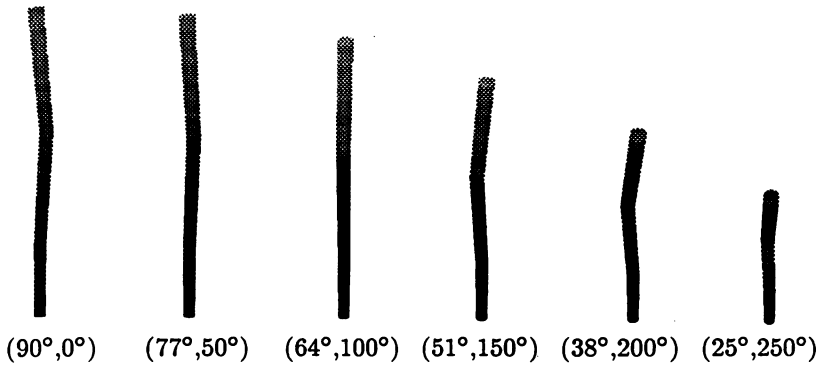
(90°,0°)   (77°,50°)   (64°,100°)   (51°,150°)   (38°,200°)   (25°,250°)

Fig. 2. The adopted jet morphology at various polar and azimuthal angles to the line of sight.

3. Results and Conclusions

Fig. 1. shows multi-epoch VLBI maps of 4C 39.25 (Marcaide *et al.* 1990) and the UMRAO monitoring data for the same period.

Fig. 2. shows the adopted jet morphology, the first panel being in the plane of the sky, with subsequent panels rotated as indicated by the labeling. The last panel – in which intensity has been rescaled to account for the Doppler boost – shows two stationary components despite the very slight nonlinearity of the flow. The top panel of Fig. 3 shows a display at intermediate epoch during the propagation of a shock, exhibiting a geometry with two stationary and one propagating component, the latter with apparent speed close to that inferred from VLBI maps. The bottom panel shows the corresponding light curves, which mimic those of Fig. 1.

The model was built to provide guidance for more detailed study, but in fact illustrates the great sensitivity of maps and light curves to orientation and flow parameters, allowing these to be well-defined with minimal effort. The model can give insight into the flow conditions: its interactive nature facilitated the exploration of parameter space, showing that opacity cannot play a significant role in determining the apparent structure of 4C 39.25 – supported by observed spectral properties. The model highlights the fact that modulation of a single outburst by flow curvature may lead to a rich light curve structure (particularly for the polarized flux) wherein (as noted by Gabuzda, private communication) there is not necessarily a one-to-one correspondence between well-defined single dish 'events' and the appearance of *new* components on VLBI maps.
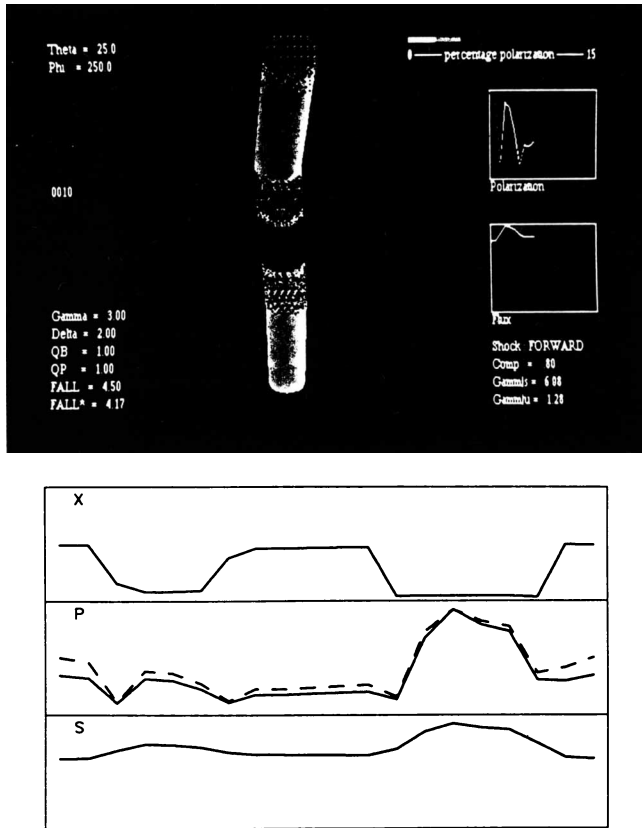
Fig. 3. Shock evolution. In the top panel the propagating component appears dark in this monochrome reproduction. The time evolution of total flux (S), polarized flux (P; percentage polarization is shown as a dashed line and reaches $\sim 5\%$) and PA of the electric vector (X) are shown in the bottom panel, and agree with those seen in Fig. 1. The early rising and late falling portions of the model light curves are presumably not seen in the data because of confusion from other outbursts.

References

Gómez, J. L., Alberdi, A., & Marcaide, J. M. 1993, *Astr. Ap.*, in press.

Hughes, P. A., Aller, H. D., & Aller, M. F. 1989, *Ap. J.*, **341**, 68.

Jones, T. W. 1988, *Ap. J.*, **332**, 678.

Marcaide, J. M., *et al.* 1990, In *Parsec Scale Radio Jets*, ed. Zensus, J. A. & Pearson, T. J. (Cambridge: Cambridge University Press), p. 59.

Marscher, A. P., Zhang, Y. F., Shaffer, D. B., Aller, H. D., & Aller, M. F. 1991, *Ap. J.*, **371**, 491.

Steffen, W. 1992. Diplomarbeit, Max-Planck-Institut für Radioastronomie, Bonn.

van der Walt, D. J. 1993, *Ap. J.*, **409**, 126.